

Article

Deep Learning-Based Joint Beamforming Design for Multi-Hop Reconfigurable Intelligent Surface (RIS)-Aided Communication Systems

Xiao Chen ^{1,*}, Jiaoyang Ye ¹, Yuxuan Wei ¹, Jianfeng Shi ² and Jianyue Zhu ²

¹ School of Artificial Intelligence, Nanjing University of Information Science and Technology, Nanjing 210044, China; 202312490773@nuist.edu.cn (J.Y.); 202412621446@nuist.edu.cn (Y.W.)

² School of Electronic and Information Engineering, Nanjing University of Information Science and Technology, Nanjing 210044, China; jianfeng.shi@nuist.edu.cn (J.S.); zhuji@nuist.edu.cn (J.Z.)

* Correspondence: x.chen@nuist.edu.cn

Abstract: Reconfigurable intelligent surface (RIS) is one of the promising technologies for sixth generation communications due to its advantages including energy saving, high spectral efficiency, etc. However, the non-convex joint beamforming design is a challenge, especially in the multi-hop RIS-assisted communication system. This paper proposes a deep learning-based joint beamforming (DLBF) design, aiming to maximize the system data rate for multi-hop RIS-aided communication systems. The proposed DLBF design consists of the reflection matrices design of all RISs and the transmit beamforming design at the base station, which has a reduced computational complexity. Numerical results show that the proposed DLBF can achieve 1.8 bit/s/Hz sum rate gain compared to the conventional beamforming method for the two-user scenario, which can be enhanced by large-scale users. The sum rate performance can be improved by increasing the number of RISs due to the reflection gain, and corresponding results provide a guidance of the multi-hop number selection for further investigation.

Keywords: reconfigurable intelligent surface; deep learning; joint beamforming; low complexity; maximum data rate



Citation: Chen, X.; Ye, J.; Wei, Y.; Shi, J.; Zhu, J. Deep Learning-Based Joint Beamforming Design for Multi-Hop Reconfigurable Intelligent Surface (RIS)-Aided Communication Systems. *Electronics* **2024**, *13*, 3570. <https://doi.org/10.3390/electronics13173570>

Academic Editor: Djuradj Budimir

Received: 23 August 2024

Revised: 6 September 2024

Accepted: 6 September 2024

Published: 8 September 2024



Copyright: © 2024 by the authors. Licensee MDPI, Basel, Switzerland. This article is an open access article distributed under the terms and conditions of the Creative Commons Attribution (CC BY) license (<https://creativecommons.org/licenses/by/4.0/>).

1. Introduction

Sixth generation (6G) communication will meet new performance indicators of future communications, including improving the data rate, expanding the communication coverage, and realizing the intelligent communication [1,2]. Reconfigurable intelligent surface (RIS) emerges as an innovative technology of 6G communication at the right moment. Specifically, an RIS is a surface consisting of massive low-cost reconfigurable passive reflecting elements, where each element can be controlled independently. An RIS can produce a reflected signal by adjusting the parameters of each element, which can reflect signal with reconfigurable amplitude and phase shift. The advanced RIS technology can effectively reduce the energy consumption as well as the hardware cost [3–6].

Existing works mainly focus on single RIS-aided communication systems, which is not available for the haul communications with significant channel blocking and signal attenuation such as the high-frequency terahertz communication. To enhance the coverage range and overcome the severe path loss, double RISs and even multiple RISs are considered. First, the double-RIS-assisted system was investigated in [7,8], where the cooperative passive beamforming design and 3D channel modeling method were proposed, respectively. Furthermore, multiple RISs were discussed in [9–11], where conventional joint beamforming designs were proposed with the goal of significantly improving the system performance such as power gain or sum rate. However, the conventional joint beamforming designs have some constraints such as high computational complexity [11] and limited convergence performance [12].

Deep learning (DL)-based neural networks were originally designed to solve classification problems, but they have also shown satisfying performance in regression problems, for example, deep neural networks (DNNs) have been used to predict transmit power [13]. For beamforming design, a DL-based transmission beamforming method was proposed based on the interrupt probability to deal with the channel uncertainty at the base station (BS) of the multiple-input single-output (MISO) downlink beamforming scenario [14]. Then, unsupervised learning was applied to beamforming design for single RIS-aided communication systems with excellent performance [15]. In [16], a DL-based joint beamforming design of transmit beamforming at the BS and phase shift design at the RIS was proposed to minimize the secrecy outage probability, which shows a lower computational complexity than the conventional methods. Therefore, our objective is to design a low-complexity DL-based joint beamforming scheme for multiple-RIS-assisted communication systems.

In this paper, a DL-based joint beamforming (DLBF) design is proposed for multi-hop RIS-enhanced multi-user communication systems, where the reflection matrices of all RISs and the transmit beamforming at BS are jointly optimized to maximize the system data rate. Furthermore, simulation results show that the proposed DLBF design achieves improved sum rate and relatively low complexity over the conventional beamforming method. The major contributions of this paper are summarized as follows:

1. In the multi-hop RIS-aided multi-user communication system, the joint beamforming design, including the reflection matrices of all RISs and the transmit beamforming for all users at BS, is a challenge. In this paper, we propose a DL-based joint beamforming scheme aiming to maximize the system data rate.
2. We analyze the computational complexity of the proposed DLBF method and the existing beamforming methods, which shows that the proposed method has suboptimal complexity performance. As a tradeoff, it is proved from the simulations that the data rate performance of the proposed DLBF method outperforms that of the existing method, having the optimal complexity performance.
3. We investigate the effect of the RIS number on the data rate performance of multi-hop RIS-aided communication systems. The simulation results prove that the data rate performance can be significantly improved by the increasing number of RISs in the low signal-to-noise ratio (SNR) scenario, while the improvement decreases even disappears in the higher-SNR scenario. Thus, the number of RISs is suggested to be adaptively set according to the SNR value of different communication systems.

2. System Model and Problem Formulation

2.1. System Model

We consider a multi-hop RIS-enhanced communication system that consists of S RISs with N_i reflecting elements for the i th RIS ($i = 1, 2, \dots, S$), K single-antenna user equipments (UEs), and one BS with M antennas. In this paper, we consider a downlink scenario, where the direct transmission channel between BS and UEs is assumed to be blocked. The reason is that the dynamic wireless environment has numerous potential obstacles and unexpected fading [10]. The cascaded BS-RIS-UE channel consists of $S + 1$ components involving three parts: first, the BS-RIS-1 channel $\mathbf{G}_{1,BS} \in \mathbb{C}^{N_1 \times M}$; second, the RIS- i -RIS- $i + 1$ channel $\mathbf{G}_{i+1,i} \in \mathbb{C}^{N_{i+1} \times N_i}$ with $i = 1, 2, \dots, S - 1$; and third, the RIS- S -UEs channel $\mathbf{H}_r = [\mathbf{h}_1 \dots \mathbf{h}_K]^T \in \mathbb{C}^{K \times N_S}$, where \mathbf{h}_k stands for the RIS- S -UE- k channel gain following the Rician fading model. The system model is shown in Figure 1. In general, RIS is deployed close to the adjacent BS or RISs that can guarantee the line-of-sight channel [10]. Here, the channel state information (CSI) is assumed to be perfectly known according to the existing channel estimation methods [17].

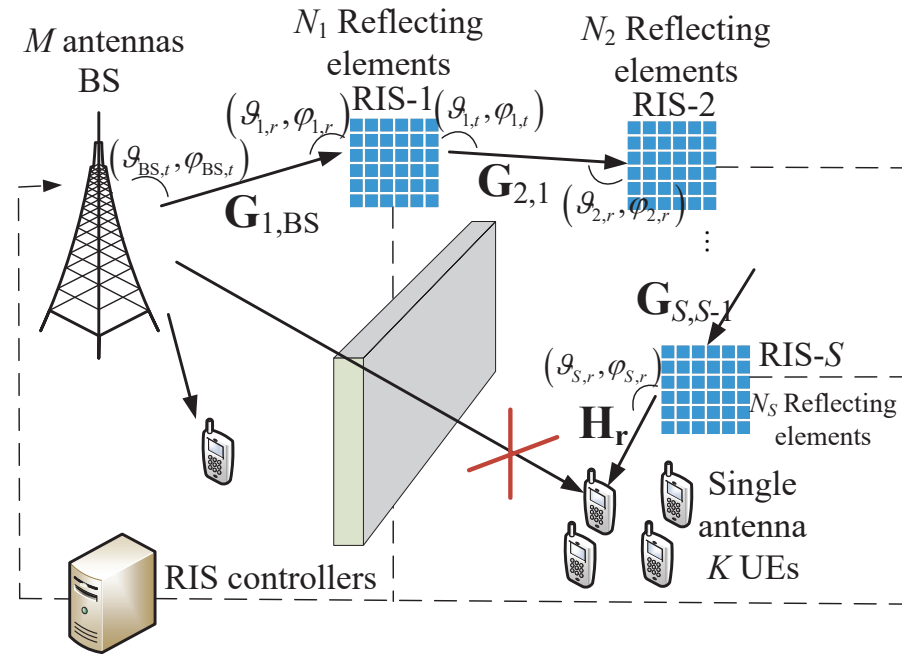


Figure 1. A multi-hop RIS-enhanced system.

The reflection matrix of the i th RIS is $\Theta_i = \text{diag}(e^{j\theta_{i,1}}, \dots, e^{j\theta_{i,n}}, \dots, e^{j\theta_{i,N_i}}) \in \mathbb{C}^{N_i \times N_i}$ ($i = 1, 2, \dots, S$), where $\theta_{i,n} \in [0, 2\pi)$ denotes the phase shift of the n th reflecting element equipped on the i th RIS. Thus, the received signal at all UEs can be given by

$$\mathbf{y} = \mathbf{H}_r \Theta_S \mathbf{G}_{S,S-1} \cdots \mathbf{G}_{2,1} \Theta_1 \mathbf{G}_{1,BS} \mathbf{W} \mathbf{s} + \mathbf{n}, \quad (1)$$

where $\mathbf{s} = [s_1, s_2, \dots, s_K]^T$ is the transmit signal with its entries satisfying zero mean and unit variance, $\mathbf{W} = [\mathbf{w}_1, \mathbf{w}_2, \dots, \mathbf{w}_K] \in \mathbb{C}^{M \times K}$ is the transmit beamforming at BS for all UEs, and $\mathbf{n} = (n_1, n_2, \dots, n_K)^T$ stands for the additive white noise vector whose entries satisfy zero mean and variance σ^2 . In the multiple-RIS-enhanced system, the BS and RIS- i are equipped with $M_x \times M_y$ and $N_{i,x} \times N_{i,y}$ uniform rectangular arrays (URAs), respectively, where $M_x M_y = M$, $N_{i,x} N_{i,y} = N_i$ ($i = 1, 2, \dots, S$), and $\{\}_x / \{\}_y$ is the number of antennas or elements in the horizontal/vertical direction of the URA. Thus, the channel matrices of BS-RIS-1 and RIS- i -RIS- $i + 1$ ($i = 1, 2, \dots, S - 1$) links can be respectively written as

$$\mathbf{G}_{1,BS} = \gamma_1 \mathbf{a}_{1,r}(\vartheta_{1,r}, \varphi_{1,r}) \mathbf{a}_{BS,t}^H(\vartheta_{BS,t}, \varphi_{BS,t}), \quad (2)$$

$$\mathbf{G}_{i+1,i} = \gamma_{i+1} \mathbf{a}_{i+1,r}(\vartheta_{i+1,r}, \varphi_{i+1,r}) \mathbf{a}_{i,t}^H(\vartheta_{i,t}, \varphi_{i,t}), \quad (3)$$

where γ_i is the complex gain, $\mathbf{a}_{BS,t}(\vartheta_{BS,t}, \varphi_{BS,t}) \in \mathbb{C}^{M \times 1}$ stands for the array steering vector of the transmission direction of BS, and $\mathbf{a}_{i,r/t}(\vartheta_{i,r/t}, \varphi_{i,r/t}) \in \mathbb{C}^{N_i \times 1}$ stands for the array steering vector of the receiving/transmission direction of RIS- i . Further, as shown in Figure 1, $\vartheta_{BS/i,t} \in [0, \pi)$ and $\varphi_{BS/i,t} \in [0, \frac{\pi}{2})$ are the azimuth and elevation angles of the BS/RIS- i 's direction-of-departure (DOD), respectively, and $\vartheta_{i,r} \in [0, \pi)$ and $\varphi_{i,r} \in [0, \frac{\pi}{2})$ are the azimuth and elevation angles of the RIS- i 's direction-of-arrival (DOA), respectively. In general, the steering vectors are given by

$$\mathbf{a}(\vartheta, \varphi) = \mathbf{a}_y(\vartheta, \varphi) \otimes \mathbf{a}_x(\vartheta, \varphi), \quad (4)$$

where $\mathbf{a}_x(\vartheta, \varphi)$ denotes an $M_x \times 1$ vector with the m_x th element being $e^{j\frac{2\pi}{\lambda} l(m_x-1) \cos \vartheta \sin \varphi}$, similarly, $\mathbf{a}_y(\vartheta, \varphi)$ denotes an $M_y \times 1$ vector with the m_y th element being $e^{j\frac{2\pi}{\lambda} l(m_y-1) \sin \vartheta \sin \varphi}$, $m_x = 1, \dots, M_x$, and $m_y = 1, \dots, M_y$, and \otimes being the Kronecker product [17]. Here, l stands for the distance between two adjacent elements or antennas of the URA, and λ is

the wavelength. To simplify the notation, let $D = \frac{2\pi}{\lambda}l$. Thus, the m th element of $\mathbf{a}(\vartheta, \varphi)$ is $[\mathbf{a}(\vartheta, \varphi)]_m = e^{jD \sin \varphi [(m_x - 1) \cos \vartheta + (m_y - 1) \sin \vartheta]}$, where $m = (m_y - 1)M_x + m_x$.

2.2. Problem Formulation

For the k th UE, the received signal is

$$\begin{aligned}
 y_k &= \mathbf{h}_k \Theta_S \mathbf{G}_{S,S-1} \cdots \mathbf{G}_{2,1} \Theta_1 \mathbf{G}_{1,BS} \mathbf{W} \mathbf{s} + n_k \\
 &= \underbrace{\mathbf{h}_k \Theta_S \mathbf{G}_{S,S-1} \cdots \mathbf{G}_{2,1} \Theta_1 \mathbf{G}_{1,BS} \mathbf{w}_k}_{\text{useful signal}} s_k \\
 &+ \underbrace{\sum_{i=1, i \neq k}^K \mathbf{h}_k \Theta_S \mathbf{G}_{S,S-1} \cdots \mathbf{G}_{2,1} \Theta_1 \mathbf{G}_{1,BS} \mathbf{w}_i}_{\text{interference signal}} s_i + \underbrace{n_k}_{\text{noise signal}},
 \end{aligned} \tag{5}$$

where $\mathbf{w}_k \in \mathbb{C}^{M \times 1}$ is the k th column of the transmission beamforming matrix \mathbf{W} at the BS. Thus, the signal-to-interference-plus-noise ratio of the k th UE can be attained

$$\gamma_k = \frac{|\mathbf{h}_k \Theta_S \mathbf{G}_{S,S-1} \cdots \mathbf{G}_{2,1} \Theta_1 \mathbf{G}_{1,BS} \mathbf{w}_k|^2}{\sum_{i \neq k}^K |\mathbf{h}_k \Theta_S \mathbf{G}_{S,S-1} \cdots \mathbf{G}_{2,1} \Theta_1 \mathbf{G}_{1,BS} \mathbf{w}_i|^2 + \sigma^2}. \tag{6}$$

Therefore, the sum data rate of all UEs can be given as

$$R = \sum_{k=1}^K \log_2(1 + \gamma_k). \tag{7}$$

The joint beamforming problem to maximize the data rate can be formulated as

$$\begin{aligned}
 \text{(P1): } & \max_{\mathbf{w}, \Theta_1, \dots, \Theta_S} R \\
 & \text{s.t. } \theta_{i,n} \in [0, 2\pi), \quad i=1, 2, \dots, S, \quad n=1, 2, \dots, N_i \\
 & \sum_{k=1}^K \|\mathbf{w}_k\|_2^2 \leq P_{max},
 \end{aligned} \tag{8}$$

where P_{max} denotes the maximum transmit power of BS. We can find that (P1) is a non-convex problem, where it is hard to obtain the optimal transmit beamforming \mathbf{W} , reflection matrices $\Theta_1, \Theta_2, \dots$, and Θ_S . Our goal is to deal with this challenging joint design problem with a reduced complexity.

3. DL-Based Joint Beamforming Design

This section discusses the DL-based joint beamforming design, including the reflection matrices design, the DNN-based equivalent beamforming design, and the decoupled design of the equivalent beamforming.

3.1. Reflection Matrix Design of RIS-1 to RIS-S – 1

We assume that the transmitting array and receiving array are far-field, and the wavefront of the narrow-band signal arriving at each element of URA is a parallel wave. According to (2) and (3), we can give the following definitions:

$$\mathbf{G}_{1,BS} = \gamma_1 \mathbf{a}_{1,r}(\vartheta_{1,r}, \varphi_{1,r}) \mathbf{a}_{BS,t}^H(\vartheta_{BS,t}, \varphi_{BS,t}) \triangleq \gamma_1 \mathbf{g}_{1,r} \mathbf{g}_{BS,t}^H \tag{9}$$

$$\mathbf{G}_{i+1,i} = \gamma_{i+1} \mathbf{a}_{i+1,r}(\vartheta_{i+1,r}, \varphi_{i+1,r}) \mathbf{a}_{i,t}^H(\vartheta_{i,t}, \varphi_{i,t}) \triangleq \gamma_{i+1} \mathbf{g}_{i+1,r} \mathbf{g}_{i,t}^H. \tag{10}$$

As a result, the received signal at the k th UE in (5) is

$$y_k = \gamma_S \mathbf{h}_k \Theta_S \mathbf{g}_{S,r} \prod_{i=S-1}^1 \gamma_i \mathbf{g}_{i,t}^H \Theta_i \mathbf{g}_{i,r} \mathbf{g}_{BS,t}^H \mathbf{W} \mathbf{s} + n_k. \tag{11}$$

Based on each element satisfying $\mathbf{g}_{i,t}^H(n) \mathbf{g}_{i,t}(n) = 1$ and $\mathbf{g}_{i,r}^H(n) \mathbf{g}_{i,r}(n) = 1$ ($n = 1, 2, \dots, N_i$), the reflection matrix of RIS- i can be designed as

$$\Theta_i = \text{diag}\{\mathbf{g}_{i,t}\} \text{diag}\{\mathbf{g}_{i,r}^H\}, \quad i = 1, 2, \dots, S - 1. \tag{12}$$

Then, by substituting (12) into (11), the received signal of the k th UE is given by

$$\begin{aligned} y_k &\stackrel{(a)}{=} \gamma_S \mathbf{h}_k \Theta_S \mathbf{g}_{S,r} \prod_{i=S-1}^1 \gamma_i N_i \mathbf{g}_{BS,t}^H \mathbf{W} \mathbf{s} + n_k \\ &\stackrel{(b)}{=} \mathcal{A} \mathbf{h}_k \Theta_S \mathbf{g}_{S,r} \mathbf{g}_{BS,t}^H \mathbf{W} \mathbf{s} + n_k, \end{aligned} \tag{13}$$

where (a) is due to $\mathbf{g}_{i,t}^H \text{diag}\{\mathbf{g}_{i,t}\} \text{diag}\{\mathbf{g}_{i,r}^H\} \mathbf{g}_{i,r} = N_i$, and (b) is achieved by the definition of $\mathcal{A} = \prod_{i=1}^{S-1} \gamma_i N_i \gamma_S$.

For simplicity, we define that $\mathbf{G} = \mathbf{g}_{S,r} \mathbf{g}_{BS,t}^H \in \mathbb{C}^{N_S \times M}$, then the cascaded channel and reflection matrix of RIS- S in (13) can be reconstructed as

$$\mathbf{h}_k \Theta_S \mathbf{G} = \mathbf{h}_k \begin{pmatrix} \mathbf{g}_1 & & & \\ & \mathbf{g}_2 & & \\ & & \ddots & \\ & & & \mathbf{g}_{N_S} \end{pmatrix} \begin{pmatrix} \Theta_{S,1} \\ \Theta_{S,2} \\ \vdots \\ \Theta_{S,N_S} \end{pmatrix}, \tag{14}$$

where $\mathbf{g}_n \in \mathbb{C}^{1 \times M}$ denotes the n th row of \mathbf{G} , and $\Theta_{S,n} = \text{diag}(e^{j\theta_{S,n}}, e^{j\theta_{S,n}}, \dots, e^{j\theta_{S,n}}) \in \mathbb{C}^{M \times M}$ consists of M elements with the same value as the n th element of the reflection matrix Θ_S of RIS- S with $n = 1, 2, \dots, N_S$. Accordingly, in (13), the equivalent cascaded channel and joint beamforming of the k th UE can be respectively given as

$$a \mathbf{h}_{eq,k} = \mathbf{h}_k \begin{pmatrix} \mathbf{g}_1 & & & \\ & \mathbf{g}_2 & & \\ & & \ddots & \\ & & & \mathbf{g}_{N_S} \end{pmatrix}, \tag{15}$$

$$\mathbf{w}_{eq,k} = \begin{pmatrix} \Theta_{S,1} \\ \Theta_{S,2} \\ \vdots \\ \Theta_{S,N_S} \end{pmatrix} \mathbf{w}_k. \tag{16}$$

Thus, the received signal at the k th UE in (13) is given by

$$y_k = \mathcal{A} \mathbf{h}_{eq,k} \left(\mathbf{w}_{eq,k} s_k + \sum_{i \neq k} \mathbf{w}_{eq,i} s_i \right) + n_k. \tag{17}$$

It can be seen that, with the known CSI in (15), the joint beamforming problem (P1) is derived as

$$\begin{aligned} \text{(P2): } & \max_{\mathbf{w}_{eq,k}} \sum_{k=1}^K \log_2 \left(1 + \frac{|\mathcal{A} \mathbf{h}_{eq,k} \mathbf{w}_{eq,k}|^2}{\sum_{i \neq k} |\mathcal{A} \mathbf{h}_{eq,k} \mathbf{w}_{eq,i}|^2 + \sigma^2} \right) \\ & \text{s.t. } \sum_{k=1}^K \frac{\|\mathbf{w}_{eq,k}\|_2^2}{N_S} \leq P_{max}. \end{aligned} \tag{18}$$

As shown in (P2), the following goal is to optimize the equivalent joint beamforming in (16) and then propose the decoupled design of the transmit beamforming \mathbf{W} and the reflection matrix of RIS-S Θ_S .

3.2. DNN-Based Equivalent Beamforming Design

The optimal equivalent joint beamforming $\mathbf{w}_{eq,k}$ can be pointed out for (P2) as [18]

$$\mathbf{w}_{eq,k} = \underbrace{\sqrt{\frac{p_{ul,k}}{N_S}}}_{\text{Power}} \underbrace{\left(\mathbf{I}_{MN_S} + \sum_{k=1}^K \frac{p_{dl,k}}{\sigma^2} \mathbf{h}_{eq,k} \mathbf{h}_{eq,k}^H \right)^{-1} \mathbf{h}_{eq,k}^H}_{\text{Direction}} \quad (19)$$

where $p_{ul,k}/p_{dl,k}$ denotes the uplink/downlink beamforming power for the k th UE, and the latter part is the beamforming direction. Thus, the goal is transformed to design the uplink and downlink power allocation \mathbf{p}_{ul} and \mathbf{p}_{dl} for all UEs.

The proposed DNN-based equivalent beamforming framework for the RIS-aided downlink system is shown in Figure 2, which is used to optimize the uplink and downlink power allocation instead of the direct beamforming estimation. To deal with the complex data, we choose the convolutional neural network (CNN) architecture since the CNN can reduce the number of learning parameters by sharing the weights and biases. As a result, the computational complexity, as well as the demand for the prediction capability in terms of network neurons and layers, is reduced significantly [13]. Moreover, CNNs demonstrate superior approximation and feature extraction abilities when compared to fully connected neural networks.

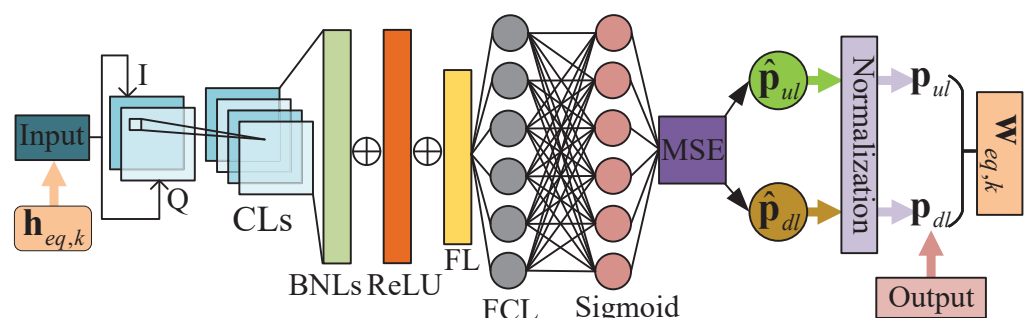


Figure 2. The DNN-based equivalent beamforming framework.

The DNN-based equivalent beamforming framework in Figure 2 consists of an input, convolutional layers (CLs), batch normalization layers (BNLs), activation layers (including ReLU and sigmoid functions), one flatten layer (FL), one fully connected layer (FCL) with $2K$ neurons, and an output. The detailed descriptions of all layers are introduced as follows.

First, the input is the equivalent cascaded channel $\mathbf{h}_{eq,k}$ in (15), where the complex channel vectors are decomposed into the in-phase component and orthogonal component, and both components contain the real part and imaginary part of the complex channel coefficients. Second, each CL creates eight convolutional kernels of size 3×3 that are convolved with the input layer, and the parameters of the convolutional kernels are shared among all channel coefficients. Third, BNLs normalize the output of the CLs, where the output of the CLs first subtracts the batch mean and then divides by the batch standard deviation, which can speed up the training process and improve the stability of the module.

As for the activation layers, the ReLU function is used in the middle, and the sigmoid function is used last since the predicted variables are positive real values and continuous. Dropout layers are added after each activation layer for randomly setting the output of a portion of neurons to zero to reduce the possibility of overfitting. After that, the FL is used to transform its input into a vector.

Furthermore, considering the continuous output values, we use the mean square error (MSE) as the loss function, which is defined as

$$\text{MSE} = \frac{1}{LT} \sum_{t=1}^T \left\| \mathbf{q}^{(t)} - \hat{\mathbf{q}}^{(t)} \right\|_2^2 \tag{20}$$

where L is the batchsize, T is the sample number, $\mathbf{q}^{(t)}$ is the target result of the t th sample in the neural network, and $\hat{\mathbf{q}}^{(t)}$ is the corresponding predicted result.

At the end, the output generates the predicted uplink/downlink power allocation vector $\hat{\mathbf{p}}_{ul}/\hat{\mathbf{p}}_{dl}$, which is normalized with the maximum transmit power constraint as

$$\begin{aligned} \mathbf{p}_{ul} &= \frac{P_{max}}{\|\hat{\mathbf{p}}_{ul}\|_1} \hat{\mathbf{p}}_{ul}, \\ \mathbf{p}_{dl} &= \frac{P_{max}}{\|\hat{\mathbf{p}}_{dl}\|_1} \hat{\mathbf{p}}_{dl}. \end{aligned} \tag{21}$$

Thus, the optimal equivalent beamforming vector $\mathbf{w}_{eq,k}$ in (19) can be attained.

3.3. Decoupled Design of Equivalent Beamforming

According to (16), the equivalent beamforming of the k th UE can be given as

$$\mathbf{w}_{eq,k} = \begin{pmatrix} \Theta_{S,1} \\ \Theta_{S,2} \\ \vdots \\ \Theta_{S,N_S} \end{pmatrix} \mathbf{w}_k = \begin{pmatrix} e^{j\theta_{S,1}} & & & & \\ & \ddots & & & \\ & & e^{j\theta_{S,1}} & & \\ & e^{j\theta_{S,2}} & & & \\ & & \ddots & & \\ & & & e^{j\theta_{S,2}} & \\ & & & & \vdots \\ e^{j\theta_{S,N_S}} & & & & \\ & & & & \ddots \\ & & & & & e^{j\theta_{S,N_S}} \end{pmatrix} \begin{pmatrix} w_{k,1} \\ w_{k,2} \\ \vdots \\ w_{k,M} \end{pmatrix} = \begin{pmatrix} e^{j\theta_{S,1}} \mathbf{w}_k \\ e^{j\theta_{S,2}} \mathbf{w}_k \\ \vdots \\ e^{j\theta_{S,N_S}} \mathbf{w}_k \end{pmatrix} = \hat{\mathbf{w}}_{eq,k} \tag{22}$$

where $\hat{\mathbf{w}}_{eq,k}$ is attained from the predicted power allocation optimized by the former DNN-based equivalent beamforming framework. It is easy to find that (22) has infinite solutions, where either particular solution is available. Thus, without loss of generality, let $e^{j\theta_{S,1}} = 1$, and general solutions for each element of the transmit beamforming \mathbf{w}_k and reflection matrix Θ_S can be obtained. For $\forall i \in \{1, 2, \dots, M\}$, we have

$$\mathbf{w}_k = \hat{\mathbf{w}}_{eq,k}(1 : M) \tag{23}$$

$$e^{j\theta_{S,n}} = \frac{\hat{\mathbf{w}}_{eq,k}((n-1)M + i)}{\mathbf{w}_k(i)}, n = 1, 2, \dots, N_S \tag{24}$$

where $\mathbf{w}_k(i)$ denotes the i th ($i = 1, 2, \dots, M$) element of $\mathbf{w}_k(i)$, and $\hat{\mathbf{w}}_{eq,k}((n-1)M + i)$ is the $((n-1)M + i)$ th element of $\hat{\mathbf{w}}_{eq,k}$.

Thus, the proposed DLBF design for RIS-assisted system can achieve the reflection matrix of RIS- i ($i = 1, 2, \dots, S-1$) in (12), the transmit beamforming of BS from (23), and the reflection matrix of RIS- S from (24). The overall algorithm to solve problem (P1) is summarized as Algorithm 1.

Algorithm 1 Proposed DLBF design.

Inputs: Transmit angles at BS ($\vartheta_{BS,t}, \varphi_{BS,t}$); azimuth and elevation angles of the RIS- i 's DOD/DOA ($\vartheta_{i,t/r}, \varphi_{i,t/r}$); the RIS-S-UE- k channel \mathbf{h}_k .

Outputs: Transmit beamforming at the BS $\mathbf{W} = [\mathbf{w}_1, \dots, \mathbf{w}_K]$; reflection matrix of the RIS- i Θ_i .

- 1: Calculate Θ_i using (12) for $i = 1, 2, \dots, S - 1$.
- 2: Update the equivalent channel $\mathbf{h}_{eq,k}$ in (15) of the k th UE.
- 3: Output the joint beamforming $\hat{\mathbf{w}}_{eq,k}$ from the DNN.
- 4: Decouple $\hat{\mathbf{w}}_{eq,k}$ into transmit beamforming \mathbf{w}_k and reflection matrix Θ_S using (23) and (24), respectively.

The computational complexity of the proposed DLBF method comes from the reflection matrix design and decoupled design of the equivalent beamforming. The complexity of the reflection matrix design in (12) is of $\mathcal{O}((S - 1)N^3)$, and in (14)–(16) is of $\mathcal{O}(N^2M + NM^2)$, where N is the number of reflecting elements of each RIS. Further, the complexity of the decoupled design in (22)–(24) is of $\mathcal{O}(NM^2)$. Thus, for K UEs, the sum computational complexity of the proposed DLBF is of $\mathcal{O}((S - 1)N^3 + K(N^2M + NM^2))$. For comparison, Table 1 summarizes the beamforming methods and corresponding complexity of the existing methods in [3,11,19,20] as well as our proposed DLBF method in this paper, where the complexity is for the one-RIS case. Table 1 shows that the proposed DLBF method has a relatively low complexity.

Table 1. The computational complexity comparison.

Literature	Beamforming Method	Complexity
[3]	Alternating optimization	$\mathcal{O}(N^6)$
[11]	Convex optimization	$\mathcal{O}(K^3 + M^4 K^{\frac{1}{2}} \log(\frac{1}{\epsilon}) I)$ ¹
[19]	Beam characteristic, ZF	$\mathcal{O}(N + K^2M + K^3)$
[20]	KKT method	$\mathcal{O}(NIK M^2)$
This paper	DL-based method	$\mathcal{O}(K(N^2M + NM^2))$

¹ Notations ϵ and I denote the solution accuracy and the number of iterations, respectively.

4. Simulation Results

This section presents the simulation results to evaluate the performance of the proposed DLBF design in multiple-RIS-enhanced multi-user systems via simulations on the TensorFlow framework based on Keras, where the simulations are running by GTX4070. In the simulations, the BS is equipped with 4 antennas, the number of UEs is $K = 2, 3, 4$, and the number of elements on each RIS is $N = 64, 100, 144, 196, 256$. The distance setting between two adjacent devices including BS, RIS and UE is 30 m, which indicates that one more RIS hop can enhance the coverage range with 30 m. In the proposed DL model, we use the Adam optimizer with the loss function in (20).

Figure 3 and Figure 4 respectively show the simulated sum data rate for 2RIS-aided systems with the number of the batch size being 50, 100, 150, and 300, and the number of training sample size being 5000, 10,000, 15,000, and 30,000, where the number of reflecting elements is $N = 64$ and the number of users is $K = 4$. First, it can be seen from both figures that the simulated sum data rate increases with the increase in SNR. Second, we can find that with the change in batch size and sample size, the simulated sum data rate does not change significantly, which indicates that the proposed model is robust.

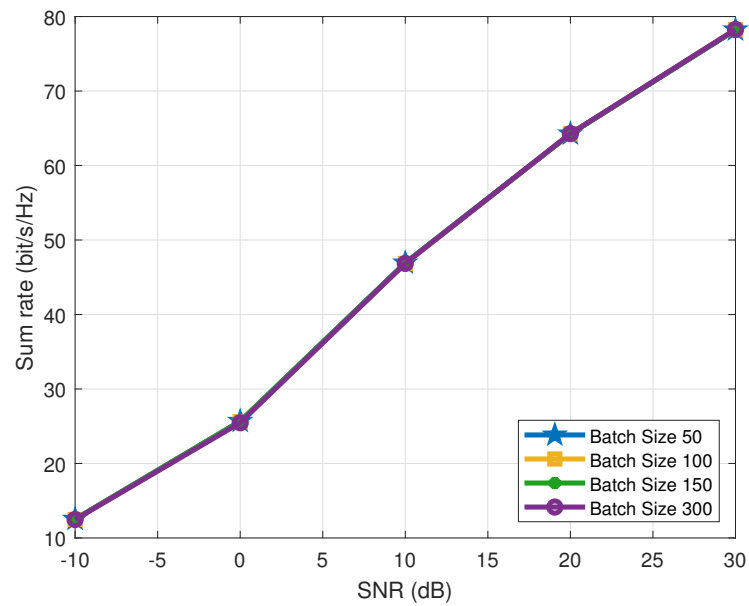


Figure 3. Simulated sum rate performance for 2RIS-aided systems with the number of batch size being 50, 100, 150, and 300.

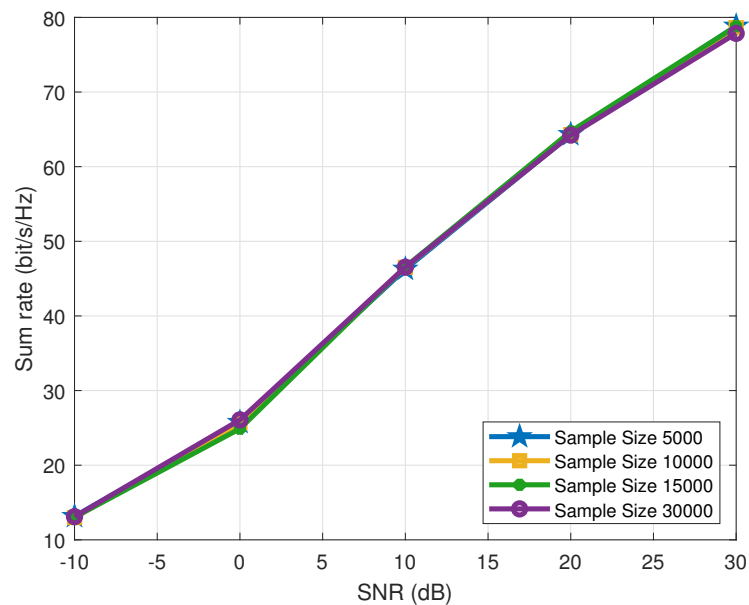


Figure 4. Simulated sum rate performance for 2RIS-aided systems with different number of training sample size.

Thus, in the following simulations, considering the calculation cost and optimal performance, we set both the epoch and batch size to be 50, where the training samples and test samples are 1×10^4 and 5×10^3 , respectively. The parameters setup of the proposed DL model is as summarized in Table 2. Notably, due to the limited precision of the phase shifter, we consider the optimized continuous phase shift (CPS), the corresponding quantized 2bit-phase shift (2PS) and 1bit-phase shift (1PS) for comparison.

Figure 5 compares the simulated sum data rate for 2RIS-aided systems, where the proposed DLBF, the conventional beamforming (BF) [19] and the random BF methods are employed for comparison, the SNR being 0 dB with $K = 2$. From Figure 5, we can see that the proposed DLBF method has about 1.8 bit/s/Hz performance gain over the conventional BF design for the 2RIS-aided system with CPS, where the performance gain can be enhanced for the large-scale UEs scenario in 6G systems. However, the data rate

performance gain of the proposed DLBF over the conventional BF in [19] is a tradeoff of the suboptimal complexity performance as shown in Table 1. For the proposed DLBF, the CPS scheme outperforms the corresponding 2PS and 1PS schemes due to the quantization error.

Table 2. Parameters for the DL model setup.

Parameter	Value
Optimizer	Adam
Loss function	MSE in (20)
Epoch	50
Batch size	50
Training samples	1×10^4
Test samples	5×10^3

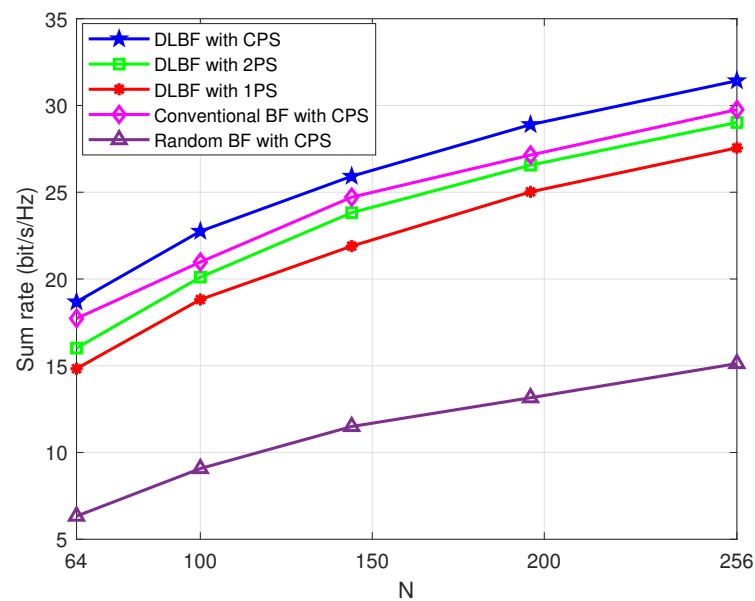


Figure 5. Simulated sum rate performance for 2RIS-aided systems with the number of reflecting elements being $N = 64, 100, 144, 196, 256$.

Figure 6 presents the simulated sum data rate for multiple-RIS-aided systems, where the number of RISs is $S = 2, 3, 4$ with $K = 2$ and $\text{SNR} = 0$ dB. Figure 6 shows that the simulated sum data rate increases with the increasing number of RISs due to the reflection gain of RIS. Further, when the number of IRSs increases from two to three, the performance gap between CPS and discrete phase shift including 2PS and 1PS is enlarged, but the performance gap between 2PS and 1PS is reduced. The reason is that more RISs bring in superimposed quantization error.

Figure 7 illustrates the simulated sum rate for multiple-RIS-aided systems employing CPS, where the number of RISs is $S = 2, 3, 4$ with $K = 2, 3, 4$ and $N = 100$. From Figure 7, it is observed that for a fixed SNR value and RIS number, the simulated sum rate performance can be improved by increasing the number of UEs. For the same number of UEs, that means all lines in the same color, the performance improvement obtained by the increasing number of RISs is decreasing with the SNR value for 2RISs and 3RISs systems, which proves that the reflection gain becomes weaker with the higher SNR. However, for the 4RISs scenario, the data rate performance outperforms that of the 2RISs/3RISs scenario in the low-SNR region but worse in the high-SNR region since with more RISs, in other words, the longer transmission distance results in serious path loss. This result provides guidance for RIS selection that, for the severe SNR scenario, it is suggested to select more RIS nodes to improve the data rate performance; for the superior SNR scenario, fewer RIS

nodes are suggested to save the total computational complexity and the achievable data rate performance.

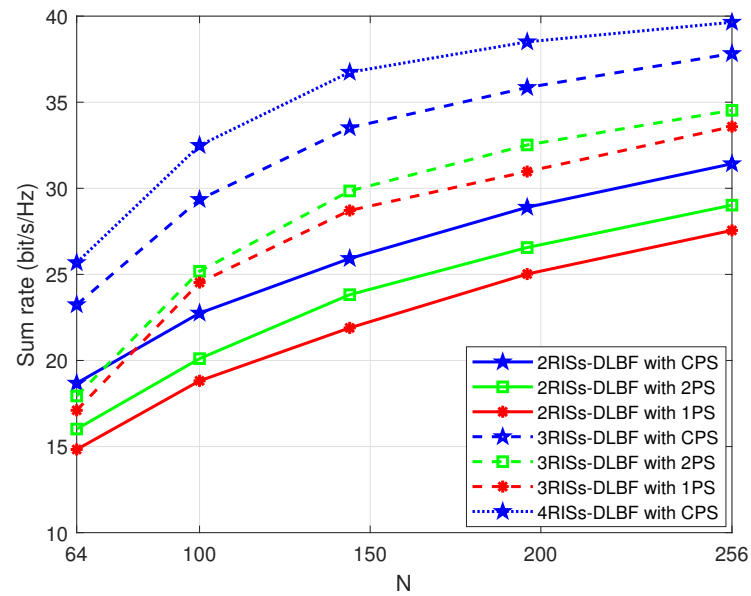


Figure 6. Simulated sum rate performance for multiple-RIS-aided systems with the number of reflecting elements being $N = 64, 100, 144, 196, 256$.

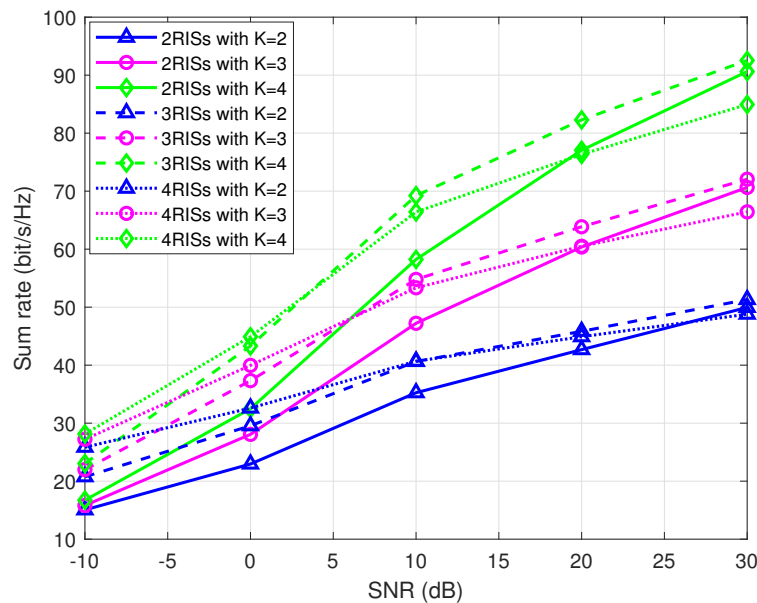


Figure 7. Simulated sum rate performance versus SNR for multiple-RIS-aided systems with the number of UEs being $K = 2, 3, 4$.

5. Conclusions

This paper proposes a DLBF design for multi-hop RIS-aided communication systems, where the reflection matrices of all RISs and the transmit beamforming at BS are optimized and formulated as closed-form expressions to maximize the system data rate. Simulation results show that the proposed DLBF design can achieve a higher sum data rate over the conventional beamforming design, which can be further enhanced by the increasing number of UEs. The simulation results prove that the data rate performance can be improved by the increasing number of RISs, while the improvement is reduced with the

increasing SNR value. Accordingly, the number of RISs in multi-hop link is suggested to be determined by the SNR value of various communication systems.

Author Contributions: Conceptualization, X.C. and J.Y.; methodology, X.C.; software, J.Y.; validation, X.C., J.Y., Y.W., J.S. and J.Z.; formal analysis, X.C. and J.Y.; investigation, X.C. and J.Y.; resources, X.C. and J.Y.; data curation, J.Y. and Y.W.; writing—original draft preparation, X.C. and J.Y.; writing—review and editing, X.C., J.Y., Y.W., J.S. and J.Z.; visualization, J.Y.; supervision, X.C.; project administration, X.C.; funding acquisition, X.C., J.S. and J.Z. All authors have read and agreed to the published version of the manuscript.

Funding: This research was funded by the National Natural Science Foundation of China, grant number 62101273 and 62201274, and the Natural Science Foundation of Jiangsu Province of China, grant number BK20220439.

Data Availability Statement: The data that support the findings of this study are available from the corresponding author upon reasonable request.

Acknowledgments: This work was supported by Xiao Chen from the School of Artificial Intelligence at Nanjing University of Information Science and Technology.

Conflicts of Interest: The authors declare no conflicts of interest.

References

1. You, X.H.; Wang, C.X.; Huang, J.; Gao, X.Q.; Zhang, Z.C.; Wang, M.; Huang, Y.M.; Zhang, C.; Jiang, Y.X.; Wang, J.H.; et al. Towards 6G wireless communication networks: Vision, enabling technologies, and new paradigm shifts. *Sci. China Inform. Sci.* **2021**, *64*, 110301. [\[CrossRef\]](#)
2. Zhang, Z.; Xiao, Y.; Ma, Z.; Xiao, M.; Ding, Z.G.; Lei, X.F.; Karagiannidis, K.G.; Fan, P.Z. 6G wireless networks: Vision, requirements, architecture, and key technologies. *IEEE Veh. Technol. Mag.* **2019**, *14*, 18–27. [\[CrossRef\]](#)
3. Wu, Q.Q.; Zhang, R. Intelligent reflecting surface enhanced wireless network via joint active and passive beamforming. *IEEE Trans. Wirel. Commun.* **2019**, *18*, 142–149. [\[CrossRef\]](#)
4. Liu, Y.W.; Liu, X.; Mu, X.D.; Hou, T.W.; Xu, J.Q.; Renzo, M.D.; Al-Dhahir, N. Reconfigurable intelligent surfaces: Principles and opportunities. *IEEE Commun. Surv. Tutorials* **2021**, *23*, 1546–1577. [\[CrossRef\]](#)
5. Pan, C.H.; Ren, H.; Wang, K.Z.; Xu, W.; Elkashlan, M.; Nallanathan, A. Hanzo, L. Multicell MIMO communications relying on intelligent reflecting surfaces. *IEEE Trans. Wirel. Commun.* **2020**, *19*, 5218–5233. [\[CrossRef\]](#)
6. Chen, Z.; Guo, Y.H.; Zhang, P.C.; Jiang, H.; Xiao, Y.H.; Huang, L. Physical layer security improvement for hybrid RIS-assisted MIMO communications. *IEEE Commun. Lett.* **2024**, *accepted*. [\[CrossRef\]](#)
7. Zheng, B.X.; You, C.S.; Zhang, R. Double-IRS assisted multi-user MIMO: Cooperative passive beamforming design. *IEEE Trans. Wirel. Commun.* **2021**, *20*, 4513–4526. [\[CrossRef\]](#)
8. Jiang, H.; Xiong, B.P.; Zhang, H.M.; Basar, E. Physics-based 3D end-to-end modeling for double-RISs assisted non-stationary UAV-to-ground communication channels. *IEEE Trans. Commun.* **2023**, *71*, 4247–4261. [\[CrossRef\]](#)
9. Huang, C.W.; Yang, Z.H.; Alexandropoulos, G.C.; Xiong, K.; Wei, L.; Yuen, C.; Zhang, Z.Y.; Debbah, M. Multi-hop RIS-empowered terahertz communications: A DRL-based hybrid beamforming design. *IEEE J. Sel. Areas Commun.* **2021**, *39*, 1663–1677. [\[CrossRef\]](#)
10. Ma, X.Y.; Fang, Y.G.; Zhang, H.X.; Guo, S.S.; Yuan, D.F. Cooperative beamforming design for multiple RIS-assisted communication systems. *IEEE Trans. Wirel. Commun.* **2022**, *21*, 10949–10963. [\[CrossRef\]](#)
11. Ma, X.Y.; Zhang, H.X.; Chen, X.H.; Fang, Y.G.; Yuan, D.F. Multi-hop multi-RIS wireless communication systems: Multi-reflection path scheduling and beamforming. *IEEE Trans. Wirel. Commun.* **2024**, *23*, 6778–6792. [\[CrossRef\]](#)
12. Yan, W.J.; Yuan, X.J.; He, Z.Q.; Kuai, X.Y. Passive beamforming and information transfer design for reconfigurable intelligent surfaces aided multiuser MIMO systems. *IEEE J. Sel. Areas Commun.* **2020**, *38*, 1793–1808. [\[CrossRef\]](#)
13. Xia, W.C.; Zheng, G.; Zhu, Y.X.; Zhang, J.; Wang, J.Z.; Petropulu, A.P. A deep learning framework for optimization of MISO downlink beamforming. *IEEE Trans. Commun.* **2020**, *68*, 1866–1880. [\[CrossRef\]](#)
14. Shi, Y.M.; Konar, A.; Sidiropoulos, N.D.; Mao, X.P.; Liu, Y.T. Learning to beamform for minimum outage. *IEEE Trans. Signal Process.* **2018**, *66*, 5180–5193. [\[CrossRef\]](#)
15. Gao, J.B.; Zhong, C.J.; Chen, X.M.; Lin, H.; Zhang, Z.Y. Unsupervised learning for passive beamforming. *IEEE Commun. Lett.* **2020**, *24*, 1052–1056. [\[CrossRef\]](#)
16. Zhang, C.; Liu, Y.L.; Chen, H.H. Deep learning based joint beamforming design in IRS-assisted secure communications. *IEEE Trans. Veh. Technol.* **2023**, *72*, 16861–16865. [\[CrossRef\]](#)
17. Chen, X.; Shi, J.F.; Yang, Z.H.; Wu, L. Low-complexity channel estimation for intelligent reflecting surface-enhanced massive MIMO. *IEEE Wirel. Commun. Lett.* **2021**, *10*, 996–1000. [\[CrossRef\]](#)
18. Björnson, E.; Bengtsson, M.; Ottersten, B. Optimal multiuser transmit beamforming: A difficult problem with a simple solution structure [lecture notes]. *IEEE Signal Process. Mag.* **2014**, *31*, 142–148. [\[CrossRef\]](#)

19. Chen, X.; Shi, J.F.; Zhu, J.Y.; Pan, C.H. General low-complexity beamforming designs for reconfigurable intelligent surface-aided multi-user systems. *J. Electron. Inform. Technol.* 2024, *in press*.
20. Almekhlafi, M.; Arfaoui, M.A.; Assi, C.; Ghayeb, A. A low complexity passive beamforming design for reconfigurable intelligent surface (RIS) in 6G networks. *IEEE Trans. Veh. Technol.* **2023**, *72*, 6309–6321. [[CrossRef](#)]

Disclaimer/Publisher’s Note: The statements, opinions and data contained in all publications are solely those of the individual author(s) and contributor(s) and not of MDPI and/or the editor(s). MDPI and/or the editor(s) disclaim responsibility for any injury to people or property resulting from any ideas, methods, instructions or products referred to in the content.